7ICMSNSE-2015

Modelling of Xe-135m for Evaluation of the CANDU6 Power Coefficient of Reactivity

Jaeha Kim¹, Yonghee Kim^{1*} and Kwangsoo Kim²

 Department of Nuclear and Quantum Engineering, Korea Advanced Institute of Science and Technology 291 Daehak-ro, Yuseong-gu, Daejeon 305-701, Republic of Korea
 Korea Hydro & Nuclear Power Co. (KHNP), 520, Yeongdong-daero, Gangnam-gu, Seoul 135-881, Republic of Korea

*Corresponding author: yongheekim.kaist.ac.kr

Abstract

There was an experimental evaluation of the PCR of a CANDU6 reactor in Korea in 2012. In the assessment, the PCR was evaluated by a methodology which requires the estimation of the reactivity variation due to Xe, liquid zone controller (LZC), etc. Unlike the conventional Xe analysis, Xe-135m was also considered in this work to estimate the total Xe worth during transient. The impact of Xe-135m on the experimental evaluation of CANDU6 PCR was evaluated based on the Xe-135m cross section data of TENDL-2014. As a result, the evaluated PCR was reduced by about 0.2 pcm/%P due to the consideration of Xe-135m.

Keywords: CANDU6, Power coefficient of reactivity, TENDL-2014, Xe-135m, Liquid zone controller, RFSP-IST, Serpent2

1. Introduction

The natural Uranium (NU) fuel results in the uniqueness of CANDU (CANada Deuterium Uranium) reactor. Heavy water (D₂O) is used as both the coolant and the moderator to utilize the natural uranium fuel for the minimization of the neutron absorption in the core. Due to the innate characteristics, it is widely accepted that the power coefficient of reactivity (PCR) of CANDU reactors is close to zero at full power condition which is resulted from its positive coolant void reactivity (CVR), positive coolant temperature coefficient (CTC), and small fuel temperature coefficient (FTC) where the PCR is the combined effect of the CTC and the FTC as in the Eq. (1). α_P is the PCR, α_{T_f} and α_{T_c} are the FTC and the CTC respectively in Eq. (1).

$$\alpha_{P} = \frac{\partial \rho}{\partial P} = \sum_{f} \left(\frac{\partial \rho}{\partial T}\right) \left(\frac{\partial T}{\partial P}\right) \cong \frac{\partial \rho}{\partial T_{f}} \frac{\partial T_{f}}{\partial P} + \frac{\partial \rho}{\partial T_{c}} \frac{\partial T_{c}}{\partial P} = \alpha_{T_{f}} \frac{\partial T_{f}}{\partial P} + \alpha_{T_{c}} \frac{\partial T_{c}}{\partial P}$$
(1)

However, the near zero PCR of CANDU reactors is undesirable since the PCR needs to be sufficiently negative to achieve the inherent stability and safety of a reactor. In this circumstances, there have been many efforts to evaluate or improve the safety parameters of CANDU reactors [1-11]. In 2012, there was a PCR assessment of a CANDU reactor, Wolseong Unit-2 in Korea, through a combination of an actual measurement during a power transient and the following core

tracking analysis which includes several reactivity variation prediction, such as the xenon reactivity [12]. Obviously, the reactivity variations need to be precisely estimated to obtain an accurate PCR value. Also, since the PCR value is very small, all factors which can affect the reactivity should be carefully considered though it has been overlooked in the conventional analysis model.

In the traditional xenon analysis contains uncertainties regarding Xe-135m that it is neglected without any assessment of its impact. Xe-135 is a main fission product which has a dominant neutron absorption cross section, so it is seriously treated in the reactor analysis while Xe-135m is neglected in the standard xenon analysis model due to its short half-life (15.29min). However, actually, the branching ratio of Xe-135m from I-135 is 16.5% and its fission yield is twice larger than that of Xe-135, so it can be non-negligible depending on its absorption cross section. According to a recent nuclear data library TENDL-2014 [13] has shown that the absorption cross section of Xe-135m is potentially even larger than that of Xe-135 though TENDL-2014 is a theoretically evaluated library without any measurement. The impact of Xe-135m with the large cross section was once briefly analyzed that the total xenon worth and the transient xenon reactivity variation will be increased by taking Xe-135m into account [14].

In this paper, the PCR of CANDU will be remeasured by the same methodology and the measurement data used in the 2012 assessment with Xe-135m being properly modeled in the xenon analysis model using TENDL-2014. Consequentially, the impact of Xe-135m on the PCR measurement will carefully be analyzed.

2. Methodologies and Models

2.1 PCR Measurement Principles

Basically, the PCR can be measured in a power transient since the PCR is the change in reactivity per unit power change. The reactivity change due to the change in temperature of coolant and fuel in a power transient is needed to be estimated to evaluate the PCR, but it cannot be directly estimated due to several accompanying reactivity factors, such as the xenon concentration change and the reactor control action. It can be known by properly canceling out the accompanying reactivity factors. This is the basic idea of the PCR measurement in this study. Figure 1 describes a power transient model in which the PCR measurement can be performed.

The reactivity variations between two critical states in a power transient are expressed in Eq.(2) where α_p is the PCR and ΔP is the power change. The reactivity variations due to xenon, other fission products, liquid zone controller (LZC) and fuel depletion are included. In CANDU, 14 LZCs in each 14 zone of the core controls the reactivity by adjusting the light water level of each compartment, so the term regarding LZC in Eq.(2) represents the reactor control action. Since the both states before and after the transient are critical, the summation of all contributing factors is zero.

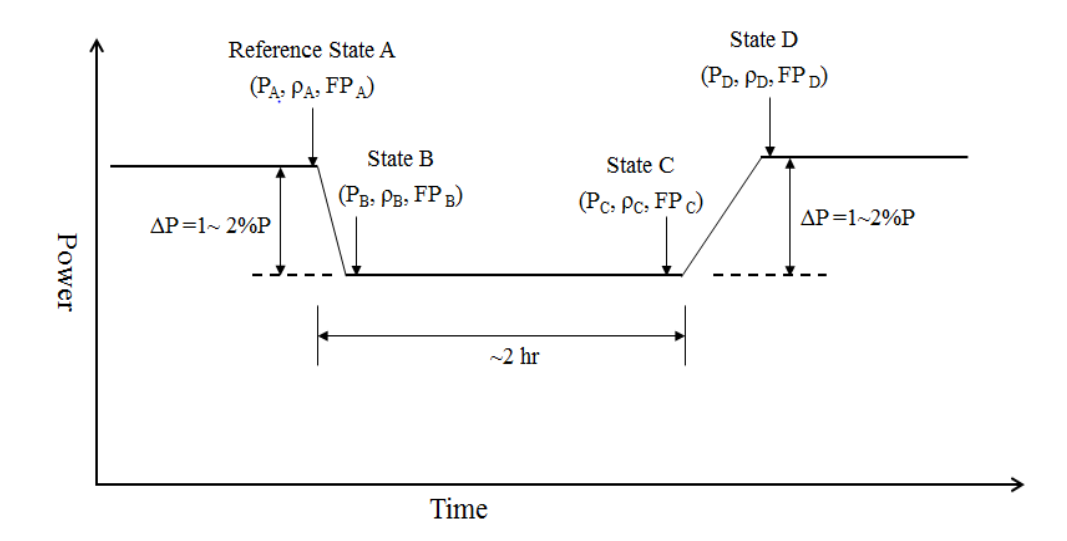


Figure 1 Power transient diagram.

$$\Delta \rho = \alpha_p \Delta P + \Delta \rho_{Xe} + \Delta \rho_{otherFP} + \Delta \rho_{IZC} + \Delta \rho_{Dep} = 0$$
 (2)

The contributions of the other minor fission products are negligible in such a short transient, Eq.(2) can be simplified and transformed as Eq.(3). The PCR was measured based on Eq.(3) by comparing the initial steady state and several specific points in time during the transient. Taking into account some merits and demerits regarding the measurement point, several points in time are selected: 5.5 min, 9 min, 15 min, and 115 min after the perturbation while the reference initial state was set to be 15 seconds before the perturbation.

$$\alpha_p = \frac{1}{\Delta P} (-\Delta \rho_{Xe} - \Delta \rho_{LZC} - \Delta \rho_{Dep}) \tag{3}$$

The actual measurement for the PCR evaluation was performed during a power transient on May 25, 2011, which includes the power level, the LZC levels and the coolant inlet and outlet temperature. The unknowns in the RHS of Eq.(3) were then estimated using following analysis models.

2.2 Analysis Models for Reactivity Estimation

The reactivity variations during the transient were estimated by several computer codes. First, the reactivity variation due to fuel depletion was simply estimated with an instantaneous core reactivity decay rate, -43.6108 pcm/FPD, obtained by RFSP-IST [15]. For the LZC reactivity estimation, RFSP-IST and a Monte Carlo code, Serpent2 [16], were both used and the results were compared. Finally for the xenon reactivity estimation, RFSP-IST and an in-house code using two-group fine-mesh finite difference method are used and compared where the in-house code. Since it is not an easy work to modify the current RFSP-IST code system to include Xe-135m, an in-house transient code was developed and utilized. In addition, though not expressed in Eq.(3), the reactivity change due to the coolant inlet temperature variation was separately corrected with the

typical CTC of CANDU reactors at full power, 4 pcm/K, since the reactivity can be affected by the coolant inlet temperature variation.

The reactor core model used in RFSP-IST is a core-tracking model which considers all the day-to-day variations while a simplified time-average model constructed by RFSP-IST is adopted in both Serpent2 and the in-house 3-D code. A time-average model is a generalized equilibrium core model which approximates the impact of everyday fuel reloading with the time-average cell properties as Eq.(4), so it gives an "average" picture of a reactor core over time.

$$\Sigma_{i,jk}(t.av.) = \frac{1}{\omega_{out,jk} - \omega_{in,jk}} \int_{\omega_{in,jk}}^{\omega_{out,k}} \Sigma_i(\omega) d\omega$$
 (4)

where ω is the fuel irradiation and $\Sigma_{i,jk}$ is a particular cross section Σ_i at position j, k. This time average model is then simplified by zone-average manner.

Table 1 shows the zone-average burnup obtained by RFSP-IST based on the core-tracking model. According to the burnup values of each zone, the fuel compositions depending on the fuel burnup were obtained by Serpent2 CANDU-6 standard lattice burnup calculation. The obtained burnup fuel compositions were then applied in the Serpent2 whole-core model [10] for the LZC reactivity estimation. All the devices and structures inside the core were properly modeled in detail in the whole-core model.

Table 1 Zone-average burnup by RFSP-IST

1 4010 1	Zone-average burnup by Kr Sr -1ST
Zone #	Average burnup (MWd/kgU)
1	3.9
2	3.8
3	3.8
4	4.3
5	3.9
6	3.6
7	3.9
8	3.8
9	3.9
10	3.8
11	4.3
12	3.8
13	3.7
14	3.8

The fuel compositions are also used in the lattice homogenization calculations to obtain two-group cell properties for the in-house code. To build the 3-D core model, 11 lattice models including the standard lattice were considered so that the effect of devices which are vertically located between fuel channels, such as the LZC compartments, the adjuster rods and the mechanical control absorber guide tube, on the cell properties can be reflected. The homogenization calculation of the 11 lattice models were performed by Serpent2.

Basically, ENDF/B-VII.0 was used in all of the Serpent2 analysis of this paper while the two-group cross section data used in RFSP-IST is generated by WIMS-IST [17] using ENDF/B-VI.

2.3 Modelling of Xe-135m

The transient Xe reactivity was evaluated by RFSP-IST and also by a two-group in-house 3-D FDM code which was verified by a nodal code MASTER [18]. In both codes, the two-group diffusion equations are solved by the finite-difference method. In RFSP-IST, the Xe transient was simulated by using *SIMULATE module so that the xenon concentration is quasi-statically tracked. Likewise, the Xe transient simulation was also performed in a quasi-static manner in the in-house code.

As shown in Figure 2, Xe-135m decays to Xe-135 with the half-life of 15.29min after produced by decay of I-135 or directly from fission. In the conventional xenon analysis model, Xe-135m is assumed to immediately decay to Xe-135 so that it is totally excluded in the xenon analysis. This assumption regarding Xe-135m leads that I-135 and Xe-135 kinetics are governed by the following equations, Eq.(5) and (6) where *I* and *X* indicates the concentration of I-135 and Xe-135, respectively. Based on these equations, I-135 and Xe-135 concentrations are explicitly tracked in RFSP-IST.

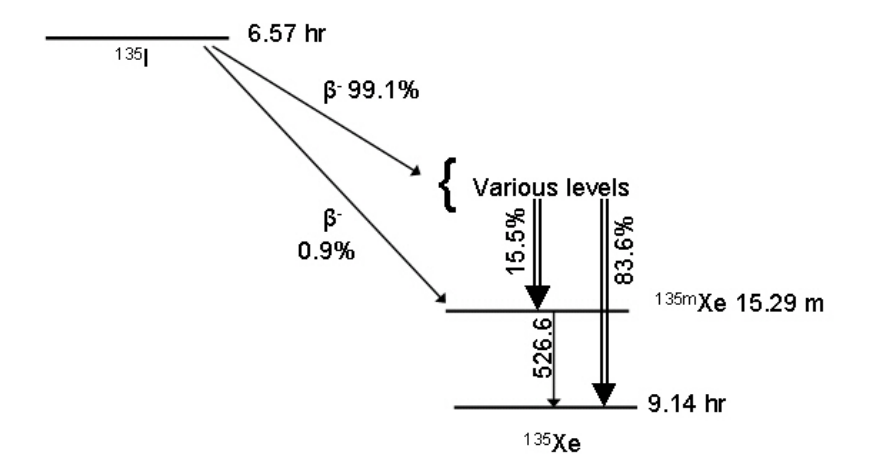


Figure 2 Decay scheme of I-135. [19]

$$\frac{dI}{dt} = \sum_{g=1}^{2} \gamma_I \Sigma_{f,g} \phi_g - \lambda_I I \tag{5}$$

$$\frac{dX}{dt} = \sum_{g=1}^{2} \gamma_X \Sigma_{f,g} \phi_g + \lambda_I I - \lambda_X X - \sum_{g=1}^{2} \sigma_X^a X \phi_g$$
 (6)

With Xe-135m being properly considered in the xenon analysis, following Eq.(7) to (9) will be the governing equations instead where *m* indicates the concentration of Xe-135m and *BR* indicates the branching ratio of Xe-135m from I-135. In the in-house code, Eq.(5) to (9) are solved numerically depending on Xe-135m option.

$$\frac{dI}{dt} = \sum_{g=1}^{2} \gamma_I \Sigma_{f,g} \phi_g - \lambda_I I \tag{7}$$

$$\frac{dm}{dt} = \sum_{g=1}^{2} \gamma_m \Sigma_{f,g} \phi_g + BR \cdot \lambda_I I - \lambda_m m - \sum_{g=1}^{2} \sigma_m^a m \phi_g$$
 (8)

$$\frac{dX}{dt} = \sum_{g=1}^{2} \gamma_X \Sigma_{f,g} \phi_g + (1 - BR) \cdot \lambda_I I + \lambda_m m - \lambda_X X - \sum_{g=1}^{2} \sigma_X^a X \phi_g$$
(9)

The required lattice parameters and the two-group capture cross section of Xe-135 and Xe-135m of the in-house code were obtained by a Monte Carlo code McCARD [20] using ENDF/B.VII.0 and TENDL-2014. In Figure 3, which compares the neutron capture cross section of Xe-135 and Xe-135m, it is noticeable that the capture cross section of Xe-135m is larger than that of Xe-135 in thermal energy range.

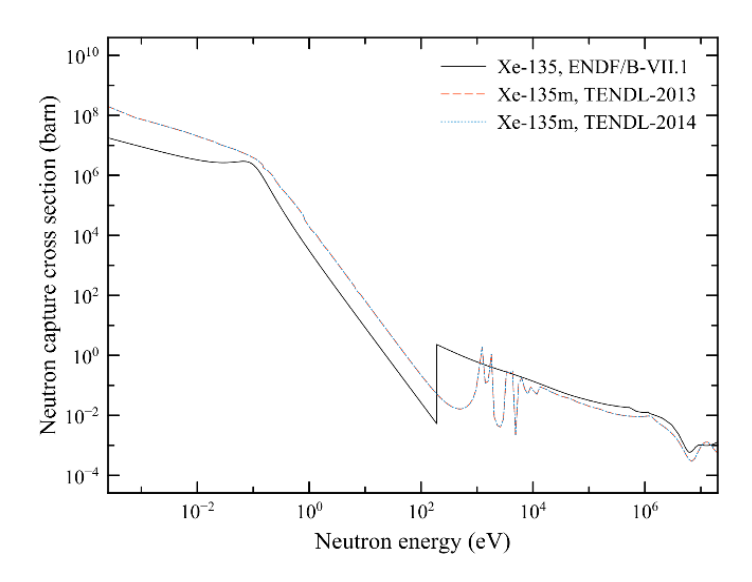


Figure 3 Neutron capture cross section of Xe-135 and Xe-135m. [13]

3. Measurement Data and Analysis

For the purpose of the PCR measurement, a power transient from full power to ~98.2 %P was carried out over 2 minutes and the reactor remained ~98.2 %P for about 2 hours from 3:00 pm to 5:00 pm. During the transient, the power level, the coolant inlet and outlet temperatures, the water level of 14 LZCs and the moderator temperature were measured on every 0.5 second. Since the data contains non-negligible white noises, the data is needed to be appropriately post-processed to determine the representative values at several points in time.

3.1 Post-processing of Measurement Data

The measurement data can be classified into two groups according to its behavior during the transient; that remains unchanged during the transient, or not. Then the data can be post-processed

according to its characteristics. The reactor power and the coolant inlet temperature are quite unchanged during the transient. In this study, the original data were simply averaged over a 30 second time window centered at a specific time of interest to determine representative values of them for the two near steady-power period. The thermal power and coolant inlet temperature data are plotted in Figure 4 (a) and (b), respectively. The power data was used in the transient Xe analysis, and the coolant inlet temperature data was used for the reactivity correction.

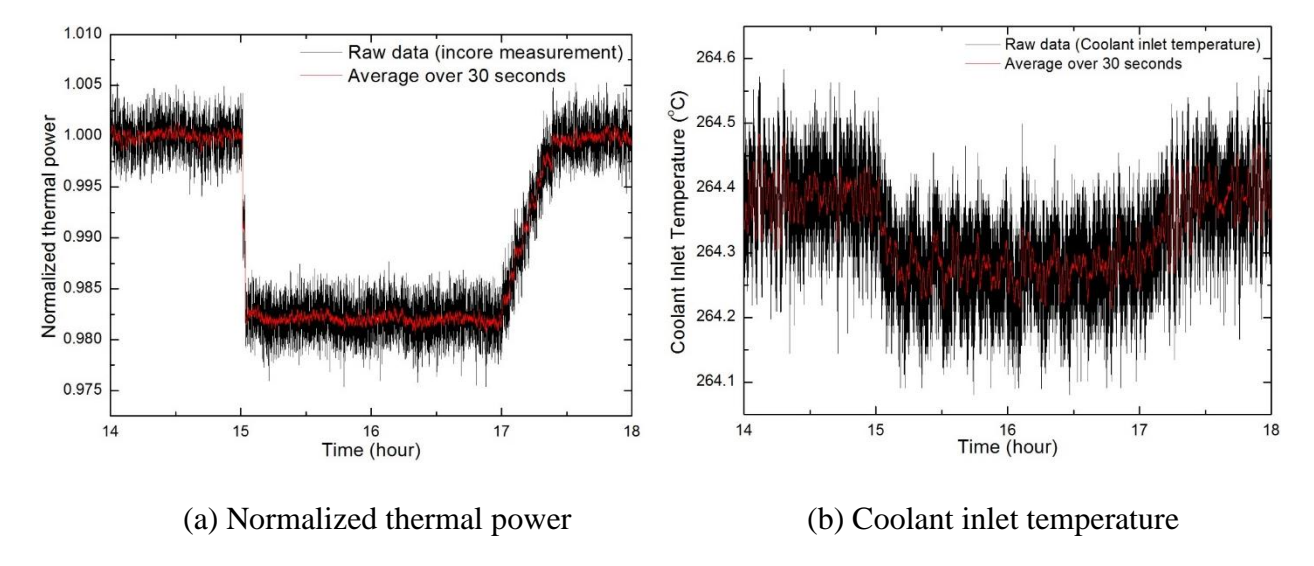


Figure 4 Measurement data during the transient

Unlike the thermal power level, the LZC levels are continuously being adjusted during the transient. Thus, the process by averaging over a specific period is not desirable for the LZC levels. In Figure 5, the time-dependent light water level data of 14 LZCs are plotted. Figure 5 shows that the water level in LZCs gradually decreases since the light water level needs to be decreased to cancel out the increase of neutron absorption by xenon during a power decrease transient.

In the measurement data, periodic and synchronized fluctuations of LZC levels on a ~10 sec period were observed, and it was found that this repetitive behavior is not just a noise, but an actual control action by reactor regulating system according to Figure 6. When the average LZC level is plotted together with the thermal power data, the correlation between them is clearly observed as in Figure 6 so that such fluctuations are believed to be actual control actions.

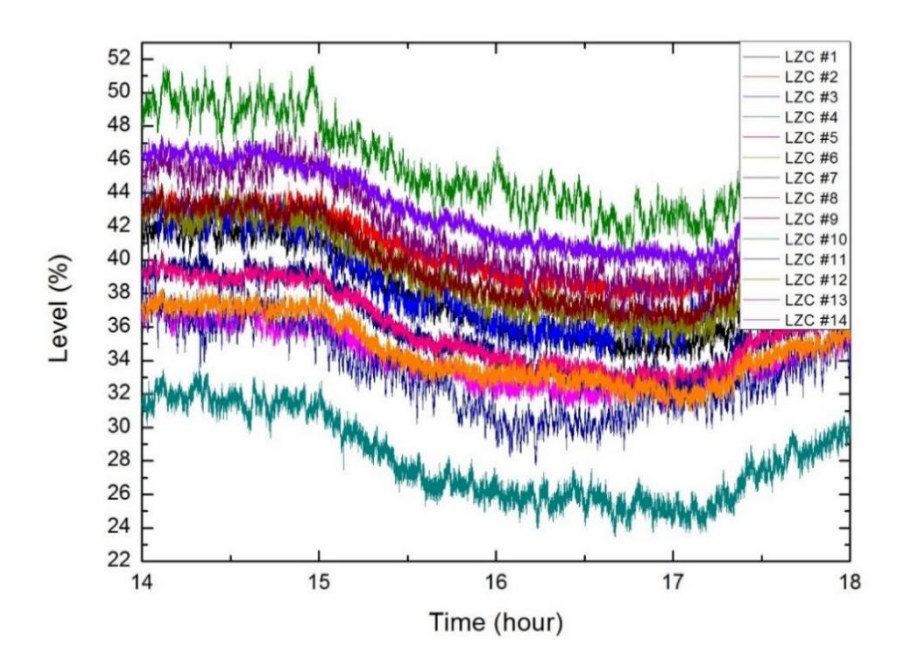


Figure 5 14 LZC level data during the transient

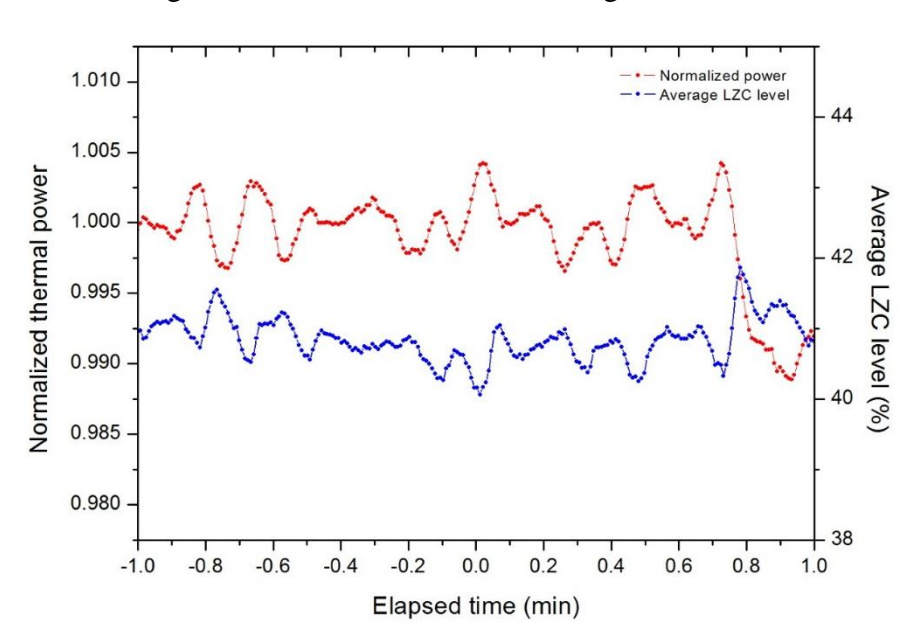


Figure 6 Correlation between reactor thermal power and the average LZC water level

Though the fluctuations are intended, it will be desirable to remove the fluctuations since the fuel and coolant temperature cannot follow such frequent actions. At this point, it can be appropriate to model the measured LZC level data as a polynomial function within a time window centered at the measurement time. In this work, a second-order polynomial regression is used to fit the measured data within a time window. Through this low-order polynomial fitting, the high frequency noises can be effectively removed. The width of the time window is set to be 60 seconds.

3.2 Reactivity Variation Estimation

The reactivity variations due to several factors during the transient were estimated based on the post-processed data and some constants. The estimated reactivity variation due to LZC, fuel depletion and coolant inlet temperature change are shown in Table 2. The estimated results of the reactivity variation due to LZC by RFSP-IST and Serpent2 whole-core model are separately presented in Table 2. Since Serpent 2 analysis is based on the Monte Carlo method, the results are not free from the statistical uncertainty. In every case of Serpent2 analysis, the standard deviation of the k-effective was ~1.06 pcm. The standard deviations were considered in the aspect of the uncertainty.

Table 2 Estimated reactivity variation

Elapsed time (min)	Estimated reactivity variation (pcm)			
	Fuel depletion, Δho_{Dep}	Coolant inlet LZC, $\Delta \mu$ temperature change,		Δho_{LZC}
		Δho_{Tin}	RFSP-IST	Serpent2
0	-	-	-	-
5.5	-0.16	-0.24	5.9	$4.77 (\pm 1.50)$
9	-0.27	-0.24	6.9	$6.86 (\pm 1.53)$
15	-0.45	-0.24	13.6	$11.03 (\pm 1.50)$
115	-3.42	-0.32	38.3	$39.96 (\pm 1.50)$

The xenon reactivity variation was evaluated by both RFSP-IST and the in-house code, and the results are presented in Table 3 and Figure 7. By the in-house code, the xenon reactivity was estimated both without and with Xe-135m. Figure 7 compares the transient xenon reactivity variation estimation by RFSP-IST and the in-house codes as a function of elapsed time and the exact results at the 5 measurement points are given in Table 3. It is clear that the two codes provide very similar xenon reactivity change during the transient when Xe-135m is not considered in the in-house code though there were some differences in the core modelling and the nuclear data used in each analysis. With Xe-135m being properly modelled, the xenon reactivity variation increases.

Based on above results regarding the reactivity variation during the transient, the PCR was evaluated according to Eq. (3).

Table 3 Transient Xe reactivity variation

Elapsed time (min)	Estimated xenon reactivity variation, $\Delta \rho_{Xe}$ (pcm)			
	RFSP-IST	In-house code		
	without Xe-135m	without Xe-135m	with Xe-135m	
0	-	-	-	
5.5	-3.5	-3.49	-3.72	
9	-5.6	-5.75	-6.09	
15	-9.7	-9.25	-9.69	
115	-31.5	-31.04	-31.34	

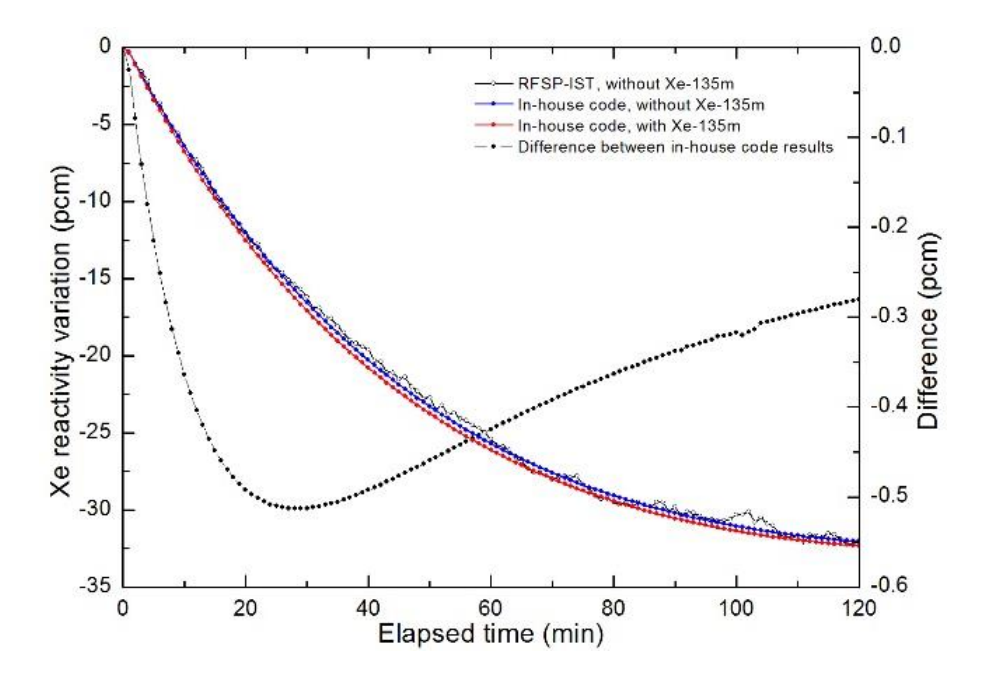


Figure 2 Estimated xenon reactivity variation

4. PCR Evaluation

The PCR of CANDU-6 was determined through the combinations of the estimated reactivity variation results by several computer codes based on the measurement data. It should be mentioned that the PCR results of this study is an approximate value for ~99 %P of the CANDU-6 reactor in an operating condition. Table 4 shows the results of PCR evaluation with the xenon reactivity estimated by RFSP-IST, in which Xe-135m is not considered while the LZC reactivity is estimated by RFSP-IST along with Serpent2. In the majority of cases, the PCR was evaluated to be clearly positive in all the cases. With the LZC reactivity estimated by Serpent2, the evaluated PCR becomes more consistent at early periods while the PCR at 115 min is exceptionally higher than in other cases, which is supposed to be due to the core condition change, such as the power distribution change over time. Thus, the average PCR value is determined without the 115 min case.

Table 4 PCR evaluation with RFSP-IST and Serpent2

	PCR (pcm/%P)		
Elapsed time (min)	RFSP-IST $(\Delta \rho_{Xe}, \Delta \rho_{LZC})$	RFSP-IST $(\Delta \rho_{Xe})$ /	
		Serpent2 ($\Delta \rho_{IZC}$)	
5.5	1.13	0.49 (±0.83)	
9	0.44	0.41 (±0.85)	
15	1.75	$0.35~(\pm 0.83)$	
115	1.62	2.51 (±0.83)	
Average*	1.10	0.42 (±0.83)	

^{*115} min case excluded

Meanwhile, Table 5 shows the results of PCR evaluation with the xenon reactivity estimated by the in-house code, with both xenon analysis models without and with Xe-135m so that the PCR evaluation results with each xenon analysis model can be compared. The overall PCR values are similar to those in the previous table since both RFSP-IST and the in-house code provide a very similar transient xenon reactivity when Xe-135m is not considered. One can note that the PCR values are decreased with Xe-135m being considered since the estimated xenon reactivity was increased with Xe-135m. Based on TENDL-2014, the PCR was decreased by about 0.19 pcm/%P.

Table 3 FCK evaluation with the in-house code and Serpent2				
Elapsed time (min) —	PCR (pcm/%P)			
	In-house $\operatorname{code}(\Delta \rho_{Xe})$ / RFSP-IST($\Delta \rho_{LZC}$)		In-house code($\Delta \rho_{Xe}$) / Serpent2($\Delta \rho_{LZC}$)	
	without Xe-135m	with Xe-135m	without Xe-135m	with Xe-135m
5.5	1.14	1.00	0.50 (±0.83)	0.36 (±0.83)
9	0.34	0.15	$0.32 (\pm 0.85)$	$0.13~(\pm 0.85)$
15	1.94	1.70	$0.54 (\pm 0.83)$	$0.30 (\pm 0.83)$
115	1.41	1.26	2.31 (±0.83)	$2.15 (\pm 0.83)$
Average*	1.14	0.95	0.45 (±0.83)	0.26 (±0.83)

Table 5 PCR evaluation with the in-house code and Serpent2

5. Conclusions

Based on measured data at Wolseong Unit 2, which is a CANDU-6 reactor, the PCR was redetermined at near full-power condition with Xe-135m being properly modelled in the xenon analysis model. For quantification of the Xe-135m impacts on the Xe reactivity and PCR, the TENDL-2014 was used and an in-house 3-D code was developed.

The results of this study consistently reveal that the PCR of CANDU6 at full power is very likely to be slightly positive, regardless of the consideration of Xe-135m. Without considering Xe-135m, the PCR was evaluated to be ~0.45 pcm/%P at 99% power, which is much smaller than the official CANDU6 PCR of ~1.7 pcm/%P at 100% power. With regard to Xe-135m, the current study clearly shows to that Xe-135m can reduce the CANDU6 PCR by about 0.19 pcm/%P with the latest TENDL-2014 library, which is non-negligible change for CANDU-6 of which the PCR is very small. Due to the limited nature of the Xe-135m nuclear data used in this work, there should be further study to quantify the uncertainty of Xe-135m data.

6. Acknowledgement

The RFSP-IST simulations and corresponding core modelling was performed by Mr. Kim, KHNP (Korea Hydro & Nuclear Power). The Serpent2 CANDU6 whole-core modelling was done by M. A. Motalab.

7. References

[1] G. Rho, "Method Development and Burnable Absorber Optimization to Improve the Power

^{*115} min case excluded

- Coefficient in the CANDU Reactor", *Ph.D. Thesis*, Korea Advanced Institute of Science and Technology, Daejeon, Republic of Korea, 2010
- [2] W. Kim, D. Hartanto and Y. Kim, "Comparative Evaluation of Fuel Temperature Coefficient of Standard and CANFLEX Fuels in CANDU 6", <u>Transaction of Korean Nuclear Society Autumn Meeting</u>, Gyeongju, Korea, October 25-26, 2012
- [3] Y. Kim, "Feasibility of Negative Power Coefficient of Reactivity on CANDU 6", <u>CANSAS</u> 2012, Daejeon, Korea, November 29-30, 2012
- [4] W. Kim, "Improvement of CANDU Safety Parameters by Using CANFLEX", *Ph.M. Thesis*, Korea Advanced Institute of Science and Technology, Daejeon, Republic of Korea, 2013
- [5] W. Kim and Y. Kim, "A Novel Utilization of Er Burnable Absorber for Improvement of CANDU Safety Parameters", <u>Trans. Am. Nucl. Soc.</u>, Vol. 108, Atlanta, Georgia, 2013
- Y. Kim and D. Hartanto, "Re-evaluation of the fuel temperature coefficient of CANDU-6", <u>Transaction of Korean Nuclear Society Autumn Meeting</u>, Gyongju, Korea, October 27-28, 2012
- [7] Y. Kim and D. Hartanto, "A High-Fidelity Monte Carlo evaluation of CANDU-6 safety parameters", PHYSOR 2012, Knoxville, Tennesse, USA, April 15-20, 2012
- [8] M. A. Motalab, W. Kim, and Y. Kim, "Investigation of the Power Coefficient of Reactivity of 3D CANDU Reactor through Detailed Monte Carlo Analysis", <u>Transaction of Korean Nuclear</u> Society Autumn Meeting, Pyeongchang, Republic of Korea, October 29-31, 2014
- [9] M. A. Motalab, D. Hartanto, and Y. Kim, "Detailed Monte Carlo Evaluation of the Power Coefficient of Reactivity of CANDU Reactor", <u>Transactions of Korean Nuclear Society Spring Meeting</u>, Jeju, Republic of Korea, May 29-30, 2014
- [10] M. A. Motalab, W. Kim, and Y. Kim, "Investigation of CANDU6 PCR with Detailed 3-D Monte Carlo Analysis", PHWR Safety 2014/CANSAS-2014, Ottawa, Ontario, Canada, June 23-26, 2014.
- [11] M. A. Motalab and Y. Kim, "Monte Carlo Evaluation of the Power Coefficient of Reactivity in 3-D CANDU Reactor", 19th Pacific Basin Nuclear Conference (PBNC 2014), Vancouver, Canada, August 24-28, 2014
- [12] Y. Kim, "Power Coefficient Assessment of CANDU Using Measurement Data", KAERI/CM-1547/2011, *The Korea Atomic Energy Research Institute*, Daejeon, Republic of Korea, 2011.
- [13] A. J. Koning, D. Rochman, "TENDL-2014", Nuclear Research and Consultancy Group (NRG), 2014
- [14] J. Kim and Y. Kim, "Preliminary Study of the Impact of Xe-135m on the PCR of CANDU", *Proceedings of PHYSOR 2014*, Kyoto, Japan, September 28 October 3, 2014.
- [15] D. A. Jenkins and B. Rouben, "Reactor Fuelling Simulation Program RFSP: User's Manual for Microcomputer Version", TTR-321, Atomic Energy of CANADA Limited, 1991.
- [16] J. Leppanen, "PSG2/Serpent a continuous-energy Monte Carlo Reactor Physics Burnup Calculation Code", VTT Technical Research Centre of Finland, 2012.
- [17] S. Douglas, "WIMS-AECL Release 2-5d User's Manual", COG-94-052 Rev. 4, July, 2000.
- [18] B.O Cho et al, "MASTER-3.0: Multi-purpose Analyzer for Static and Transient Effects of Reactors", KAERI/TR-2061/2002, *The Korea Atomic Energy Research Institute*, Daejeon, Republic of Korea, 2012
- [19] J.K. Hartwell, D.M. Scates, J.B. Walter, and M.W. Drigert, Determination of the Quantity of I-135 Released from the AGR-1 Test Fuels at the End of ATR Operating Cycle 138B, Idaho National Laboratory, p.2, 2007.
- [20] H. J. Shim and C. H. Kim, "McCARD User's Manual", Version 1.0, Nuclear Design and Analysis Laboratory, Seoul National University, 2010.